Optical spectra of lithium vapour zones produced by thermal evaporation in hydrogenating atmosphere

Optical spectra of lithium vapour zones produced by thermal evaporation in hydrogenating atmosphere

Shosuke Mochizuki†, Mie Sasaki‡ and Raphael Ruppin§

Department of Physics, College of Humanities and Sciences, Nihon University,
3-25-40 Sakurajosui, Setagaya-ku, Tokyo 156-8550, Japan

Abstract. We have applied the time-resolved and space-resolved spectroscopies of vapour zones produced by gradual thermal evaporation in a noble gas to study the electronic properties and stability of hydrogenated clusters and microcrystals. Optical extinction spectra of lithium vapour zones in pure Ar gas and Ar–H_2 gas mixture atmospheres confined at various pressures were obtained. Some comparisons of the observed spectra with those predicted theoretically indicate that hydrogenated clusters $Li_n H_m$ are to be found near the vapour source, while lithium microcrystals coated with LiH shells are to be found far away from the vapour source. Electron localization around hydrogen atoms and the hydrogenation mechanism of lithium particles are also discussed.

1. Introduction

Recently, there has been growing interest in the hydrogenation of metal clusters and microcrystals, because the system $M_n H_m$ (M = metal atom) may exhibit different physical and chemical properties with progressing hydrogenation. However, the following basic problems still remain to be clarified.

(1) How do evaporated metal atoms interact with other atoms and atmospheric hydrogen gas to grow clusters and microcrystals, and become hydrogenated?

(2) What are the atomic structures of hydrogenation products?

(3) Which is more stable: uniformly hydrogenated product $M_n H_m$ clusters (Vezin *et al* 1993a, Antoine *et al* 1997) or hydride-coated metal ones which consist of $M_x H_m$ shell and M_{n-x} core, for a given system size and temperature?

(4) How does the hydrogenation localize some of the valence electrons in clusters around the hydrogen atoms and affect the collective mode resonance of these valence electrons and the optical properties?

In order to elucidate these problems, lithium is chosen for the present study because it is the lightest metal. This makes it easier to investigate from a theoretical point of view. Also, the clusters and microcrystals exhibit a very clear collective mode resonance for which the resonance wavelength, bandwidth and spectral shape are sensitive to the shape, electronic structure and atomic structure of the relevant system. For the present purpose, it is best to

produce a free cluster stream that contains size-selected hydrogenated clusters and to measure the photoabsorption cross section spectra and other physical properties as functions of size and composition, $M_n H_m$, as done by Vezin *et al* (1993b) and Antoine *et al* (1997). Recently, we have produced two vertically well separated zones of lithium vapour above the evaporation source in a confined noble gas atmosphere by setting an appropriate condition for the gas evaporation (Mochizuki *et al* 1997). Optical extinction spectra of lithium atoms, dimers and clusters were obtained by time-resolved and space-resolved measurements after the beginning of the evaporation. Here, we expand these optical studies to the investigation of the hydrogenated lithium clusters and microcrystals. The main limitation of our technique is that there is no direct characterization of the cluster size, *in situ*. Bearing this limitation in mind, we will present some reasonable connection between measured optical data and hydrogenation effects in lithium clusters and microcrystals.

2. Experiment

Gas evaporation experiments were carried out in pure Ar gas and in Ar–10% H_2 mixture gas confined at various pressures from 30 Torr to 150 Torr using the apparatus described earlier (Mochizuki *et al* 1997). A stainless steel crucible containing nominally pure lithium metal was gradually heated indirectly in an alumina crucible on which a tungsten-wire heater was wound. The temperature of the crucible increases with time elapsed after the beginning of heating and, therefore, the concentration of evaporated lithium atoms also increases with time. The transmissivity spectra of selected positions in the vapour and beam zones were recorded as a function of time elapsed after the beginning of the evaporation as follows. Continuum light from a 150 W Xe lamp was directed at the whole vapour zone or beam zone through an optical window without using any lens. After passing the vapour zone, only the light through a selected position was collected by a lens and then introduced into an optical multichannel analyser through an optical fibre. The transmissivity T_r at a given height is the intensity ratio of the transmitted radiation during gas evaporation to that of transmitted radiation through the same position before the beginning of the evaporation. Since the transmissivity spectra T_r obtained in the vapour-zone measurements contain the effects of both scattering and absorption, the results obtained are expressed as extinction spectra $- \log T_r$. In the experiments, we determined the temperatures of the vapour zones with a thermocouple as functions of height and time elapsed after starting of heating.

3. Results and discussion

3.1. Optical extinction of faint dark red vapour zone

As reported in the previous paper (Mochizuki *et al* 1997) on the gas evaporation of lithium, two vertically well separated zones of lithium vapour appear above the evaporation source in a confined noble gas atmosphere by setting an appropriate condition for the gas evaporation. Under an Xe lamp illumination a faint dark red zone, ranging from the upper edge of the crucible to a height of about 5 mm, and a long conical blue zone appeared. Each zone size depends on the atmospheric gas pressure and the temperature of the crucible. The faint dark red and blue colours correspond to the fluorescence of lithium atoms and the collective mode resonance scattering of lithium clusters, respectively. As the gas evaporation proceeds, the blue zone grows to produce a multi-layer cone structure. Such a vapour zone structure was also observed in a confined Ar–H_2 mixture gas atmosphere. However, unlike the Ar gas case, here the inner part of the multi-layer conical zone becomes slightly whitish blue in colour.
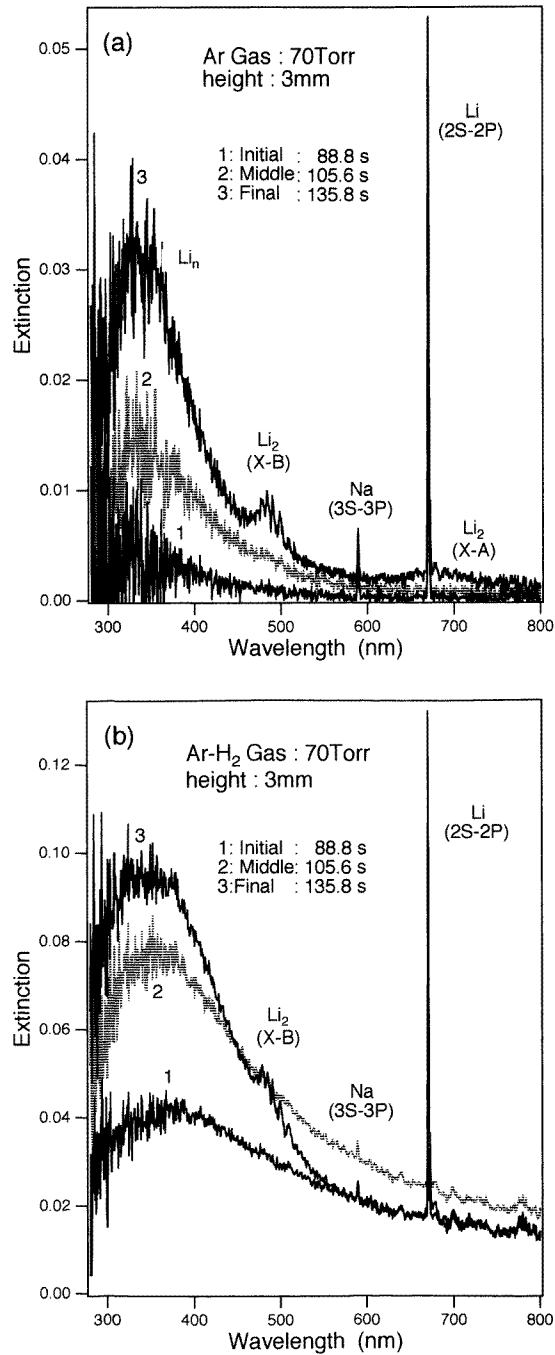
Figure 1. Evolution of the extinction spectra of lithium vapour zone at a height of 3 mm: (a) in Ar gas atmosphere, (b) in Ar–H$_2$ mixture gas atmosphere.

We have measured the time evolution of the extinction spectrum of the faint dark red zone at a height of 3 mm from the crucible edge in Ar gas confined at 70 Torr. Of the 64 spectra

measured at time intervals of 980 ms, typical ones at the initial, middle and final stages of the gas evaporation are shown in figure 1(a). The times indicated are the those elapsed after the beginning of heating. During the measurements, the temperature of the measured zone rose from 502 K to about 702 K, over a time of about two minutes. At the initial stage of gas evaporation, only a sharp absorption line due to lithium atoms appears at about 670.7 nm. This wavelength is close to the reported value (White 1934, Phelps 1982) of the 2S–2P electronic transition in atomic lithium. With evaporation in progress, broad absorption bands with fine structures appear at wavelength regions from 600 nm to 800 nm and from 450 nm to 550 nm. By referring to a spectroscopic table (Rosen 1970), the former and the latter are assigned to the X–A and X–B electronic–vibrational transitions in the lithium dimer Li_2, respectively. Also, another very broad band is observed around 334 nm. This band is assigned to the collective mode resonance of valence electrons in lithium clusters Li_n ($n > 2$). Since the vapour zone at 3 mm was almost transparent, it may be assumed that the lithium clusters in this zone are not microcrystals but clusters. In these spectra, the D line of impurity sodium appears at about 589 nm.

We have also measured the time evolution of the extinction spectrum of the faint dark red zone at a height of 3 mm from the crucible edge in Ar–H_2 mixture gas confined at 70 Torr, as 64 time-resolved spectra. In figure 1(b), typical spectra at the initial, middle and final stages of the gas evaporation are shown. The times indicated are the those elapsed after the beginning of heating. During the measurements, the temperatures of the measured zone rose from about 533 K to about 722 K. The temperature increase observed under the gas mixture is due to the addition of H_2 gas whose thermal conductivity is about ten times that of Ar gas. As seen in these figures, at the initial and middle stages, the spectra are characterized by the atomic absorption at 670.7 nm. We could not observe the X–A and X–B absorptions due to LiH dimers at reported wavelength regions, between 430 nm and 340 nm and between 308 nm to 288 nm, respectively (Rosen 1970). We therefore conclude that there are only a few LiH dimers, so that their absorptions are obscured by the collective mode band. Comparing these experimental results with those observed in pure Ar gas atmospheres, we see that the extinction due to atoms is about doubled when Ar gas is replaced by Ar–H_2 mixture. The temperatures of the measured vapour zone at the final stage of evaporation in Ar and Ar–H_2 gas atmospheres were 702 and 722 K, respectively. The temperature $T(K)$ dependence of lithium vapour pressure P (Pa) (Yoshikawa 1989),

$$\log P = -(8415/T) + 11.34 - 1.0 \log T + 2.125 \tag{1}$$

shows that a temperature increase of 20 K may give about twice the concentration of evaporated lithium atoms, which would explain the observed absorption intensity increase. Also, the collective mode resonance is broader than in the pure Ar gas case. The collective mode resonance is observed at 370 nm at the initial stage of evaporation and it shifts to shorter wavelength (344 nm) with progressing gas evaporation. This blueshift may be ascribed to the depression of the electron spillout effect in larger clusters. Approaching the final stage, the absorption due to the X–B electronic–vibrational transition in lithium dimers becomes observed around about 490 nm, which may result from some thermal decomposition of Li_nH_m clusters, because of the temperature increase with time. It should also be noted that, when the absorption due to dimers appeared, the extinction was depressed at wavelengths longer than about 550 nm. The appearance of lithium dimers is accompanied by the spectral narrowing of the collective mode resonance and, therefore, the following thermal decomposition of hydrogenated clusters,

$$Li_nH_m \rightarrow Li_{n-2}H_{m-2} + Li_2 + H_2 \tag{2}$$

may occur to produce clusters of higher symmetry. The $Li_{n-2}H_{m-2}$ clusters may be more stable clusters of magic numbers.
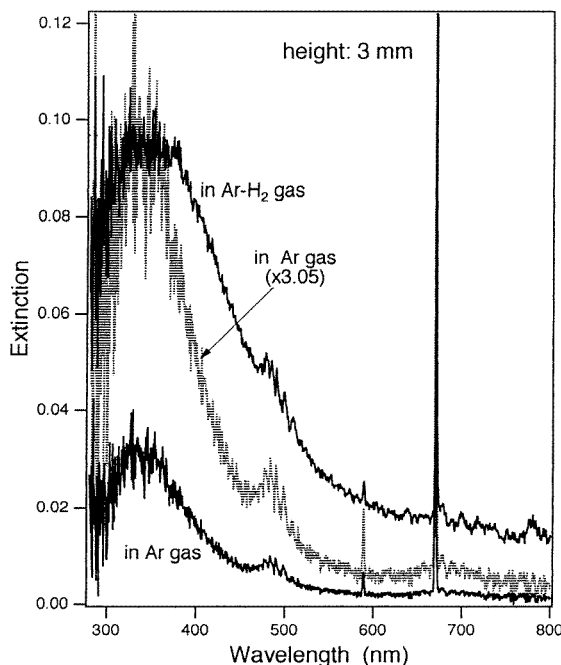
Figure 2. Spectral changes caused by replacing Ar gas by Ar–H$_2$ mixture.

In figure 2, the spectrum observed at the final stage of evaporation in Ar gas atmosphere is compared with that observed in the Ar–H$_2$ gas one at the final stage of evaporation. They are normalized with respect to the intensity at the peak wavelength. It is found that the extinction intensity of the collective mode resonance was tripled by replacing Ar gas by Ar–H$_2$ gas, while the emission intensity of atoms was increased two and half times. Preferential production of hydrogenated lithium clusters in the faint dark red zone in the Ar–H$_2$ gas atmosphere may be confirmed by the spectral features of figure 1(b), namely, the extinction intensity increase, the blueshift to the highest collective resonance wavelength (about 334 nm) of pure lithium clusters, the appearance of the longer wavelength tail of the collective mode resonance (Vezin *et al* 1993b) and the disappearance of absorption due to dimers. The observed spectral broadening of the collective mode resonance in Li$_n$H$_m$ clusters may be explained by the geometrical structure with lower symmetry than lithium clusters, or by some resonance scattering of delocalized electrons by electrons localized around hydrogen atoms. Vezin *et al* (1993b) interpreted their photodepletion spectra of Li$_n$H in terms of the first of these explanations. An explanation in terms of resonance scattering is analogous to the virtual bound state model of d electrons in transition and noble metals (Friedel 1954). We assume that the delocalized state is separated from the localized one by some thin potential barrier. In such a case, electrons move between the delocalized state and virtual bound states of hydrogen atoms through the potential barrier by quantum-mechanical tunnelling, thereby suffering scattering.

3.2. Optical extinction of blue and whitish-blue vapour zone

The time evolution of the extinction spectrum of the blue zone was measured at a height of 20 mm from the crucible edge in Ar gas confined at 70 Torr. In figure 3(a), the spectra at the initial, middle and final stages of gas evaporation are shown. During the measurements, the temperature of the measured zone rose up to 534 K.
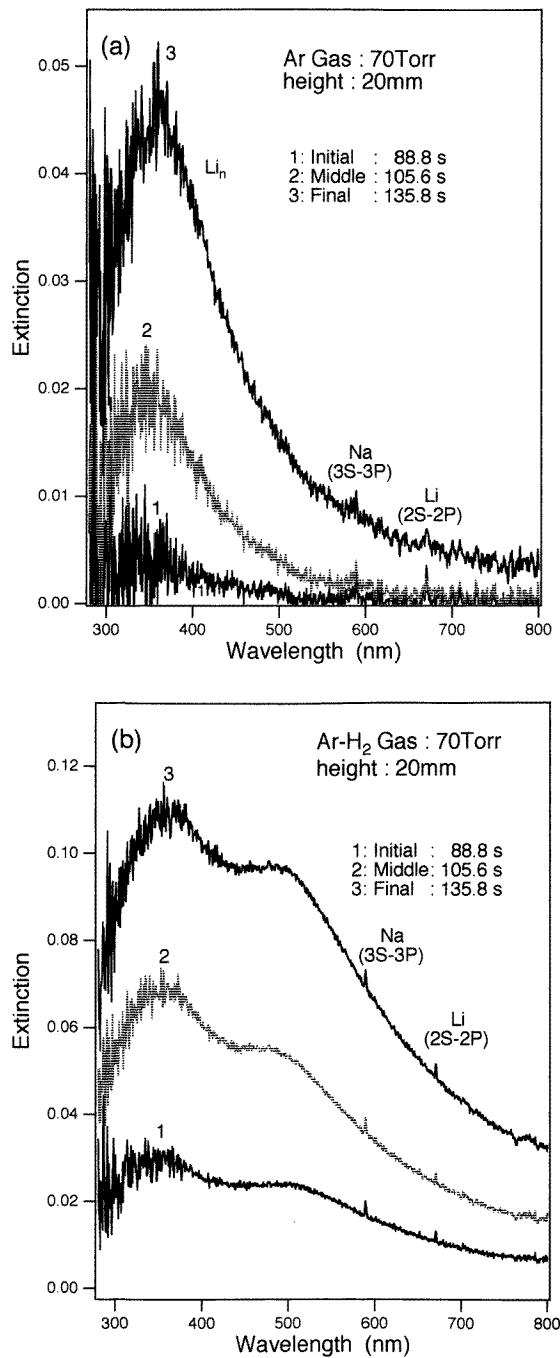
Figure 3. Evolution of the extinction spectra of lithium vapour zone at a height of 20 mm: (a) in Ar gas atmosphere, (b) in Ar–H$_2$ mixture gas atmosphere.

The time evolution of the extinction spectrum of the whitish-blue zone was measured at a height of 20 mm from the crucible edge in Ar–H$_2$ gas mixture confined at 70 Torr.
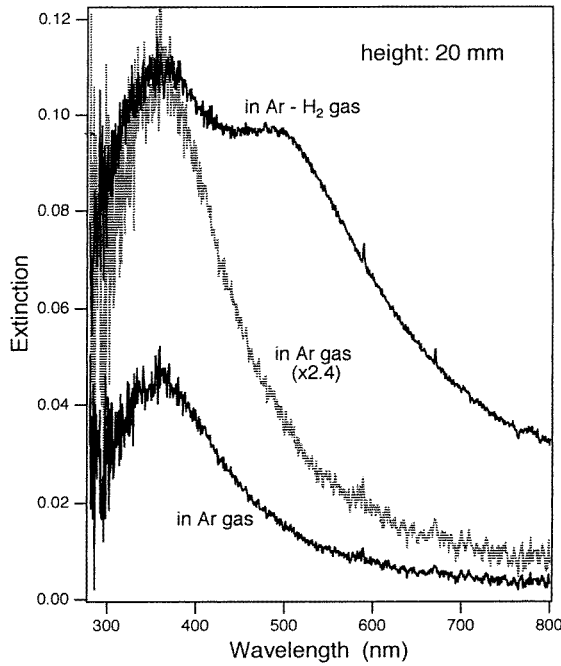
Figure 4. Spectral changes caused by replacing Ar gas by Ar–H$_2$ mixture.

In figure 3(b), the spectra at the initial, middle and final stages of gas evaporation are shown. During the measurements, the measured zone temperature rose up to 542 K. As seen in the spectra, in addition to the collective mode resonance absorption observed at about 340 nm as in pure lithium microcrystals, another new absorption band appeared at about 500 nm. The spectra observed in Ar gas and Ar–H$_2$ gas mixture atmospheres at their final stage are shown in figure 4. We also measured the time evolution of the extinction spectrum at different pressures ranging from 30 Torr to 150 Torr. The spectra observed at the final stage are shown in figure 5(a). The temperatures of the measured position at the pressures 30, 70, 110 and 150 Torr were 536, 542, 547 and 555 K, respectively. With increasing pressure, the new band buried in the collective mode resonance of lithium microcrystals shifts to longer wavelength to give a double band structure in the spectra. Because, unfortunately, we have no method for determining the sizes and structures of such free microcrystals *in situ*, we tried to simulate the observed spectra by calculating the extinction cross section of spherical microcrystals, as in previous studies (Mochizuki *et al* 1997). In the calculation, we assume that there co-existed pure lithium spherical microcrystals (R: radius) and LiH-coated spherical lithium ones (R_1: radius of lithium core, R_2: outer radius of LiH shell) with the same diameters $R(= R_2)$ in the whitish-blue zone. The extinction of the LiH-coated Li spheres was calculated from the general scattering theory for stratified spheres (Kerker 1969). For these calculations, we have employed the values of the frequency dependent complex dielectric constant of lithium as measured by Inagaki *et al* (1976). These, however, refer to the bulk, and for small spheres they have to be modified so as to account for the free-path effect, which leads to an increase of the imaginary part of the dielectric constant. For this size dependent correction the form suggested by Kreibig (1974) has been used. For the dielectric constant of LiH, the value 3.61 has been used (Iida *et al* 1972). In the calculations we have varied the sphere and shell sizes, until the peak positions agreed with those of the curves shown in figure 5(a). In figure 5(b),
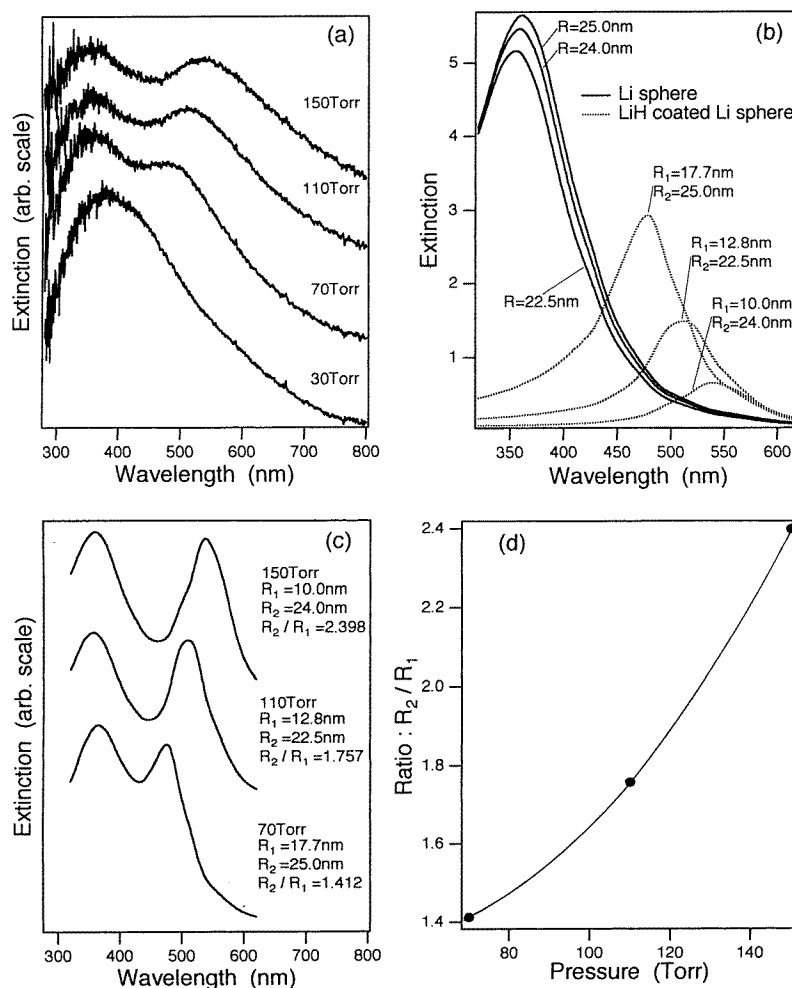
Figure 5. Ar–H_2 gas pressure dependence of the extinction spectrum of whitish-blue zone: (a) experimental spectra, (b) calculated ones, (c) simulation of experimental spectra by scaled combinations of spheres and coated spheres, (d) pressure dependence of R_2/R_1.

the solid and dotted curves correspond respectively to pure lithium spheres and LiH-coated Li spheres with the same outer radii R which are indicated on each curve. The extinction cross sections are expressed in units of the geometrical cross section. It is found in the calculations that, with increasing thickness of the LiH shell, the low energy extinction peak shifts to longer wavelength and its intensity decreases. The experimental spectra of figure 5(a) are simulated by assuming that pure Li spheres coexist with LiH-coated Li spheres having the same external radius. We have thus combined appropriate pairs of calculated spectra of figure 5(b), so that the relative heights of the two maxima will agree with the experimental intensity ratios. The result is shown in figure 5(c) and the Ar–H_2 gas pressure dependence of the ratio R_2/R_1 is shown in figure 5(d). Therefore, the increase of Ar–H_2 gas pressure promotes hydrogenation on the surfaces of lithium microcrystals to produce LiH shells. It is also concluded that, in the microcrystal size region, the structure consisting of a LiH shell and pure lithium core is more stable than that of uniformly hydrogenated microcrystals.

3.3. Hydrogenation of clusters and microcrystals

Now, we discuss the way in which evaporated metal atoms interact with other atoms and atmospheric gas to grow clusters and microcrystals as well as to be hydrogenated under an H_2 atmosphere. We note the absorption intensity of the atomic line shown in figures 1(a) and (b). Since, as pointed out in section 3.1, the doubling of the atomic absorption intensity when replacing Ar gas by Ar–H_2 gas atmosphere arises from a pure temperature effect, the number of atoms in the dark zone is thought to be uninfluenced by hydrogenation at the same evaporation temperature, which indicates the unexpectedly high stability of lithium atoms even in the present evaporation condition in a hydrogenating atmosphere. On the other hand, the peak wavelength of the extinction intensity due to clusters is also nearly independent of hydrogenation, but considerably affected in the spectral shape by hydrogenation. Generally, the extinction peak wavelength depends on cluster size. Since the extinction peak frequency of collective mode resonance observed in Ar–H_2 gas atmosphere is close to that observed in the pure Ar one, we assume that the average cluster size is not greatly changed by replacing Ar gas by Ar–H_2 gas. This indicates that lithium clusters are first produced and then they react with H_2 gas molecules to produce Li_nH_m clusters. For such hydrogenation of lithium clusters, a possible process is the adsorption accompanied by dissociation of H_2 molecules approaching the cluster surfaces, similar to that proposed for the hydrogenation of solid metal by Lennard-Jones (1932) a long time ago.

4. Final remarks

To observe a typical hydrogenation effect, we evaporated lithium under various pressures of a 90% Ar–10% H_2 mixture gas besides Ar gas in the present study. However, varying the partial pressure of H_2 gas and replacing Ar gas by another kind of noble gas may influence the temperatures of the vapour zones and the mean free path of the evaporated species and, as a result, change the average cluster size. Therefore, it is interesting to carry out the optical measurements under various kinds of hydrogen–noble gas mixture as a function of partial pressure of H_2 gas for more detailed study. Such experiments are now in progress in our laboratory.

References

Antoine R, Dugourd Ph, Rayane D, Benichou E, Vezin B and Broyer M 1997 *Z. Phys.* D **40** 436
Friedel J 1954 *Adv. Phys.* **3** 446
Iida S, Ohno K, Kanzaki H, Kumagaya H and Sawada S 1972 *Butsuri Teisuuhyou* (Tokyo: Asakura Syoten) (in Japanese)
Inagaki T, Emerson L C, Arakawa E T and Williams M W 1976 *Phys. Rev.* B **13** 2305
Kerker M 1969 *The Scattering of Light and Other Electromagnetic Radiation* (New York: Academic)
Kreibig U 1974 *J. Phys. F: Met. Phys.* **4** 999
Lennard-Jones J E 1932 *Trans. Faraday Soc.* **28** 333
Mochizuki S, Sasaki M and Ruppin R 1997 *J. Phys.: Condens. Matter* **9** 5801
Phelps III F M 1982 *M.I.T. Wavelength Tables* (Cambridge, MA: MIT Press)
Rosen B 1970 *Spectroscopic Data Relative to Diatomic Molecules* (Oxford: Pergamon)
Vezin B, Dugourd Ph, Rayane D, Labastie P, Bordas C and Broyer M 1993a *Z. Phys.* D **26** S128
——1993b *Z. Phys.* D **26** 290
White H E 1934 *Introduction to Atomic Spectra* (New York: McGraw-Hill)
Yoshikawa H 1989 *Sinkuu Handbook* (Tokyo: ULVAC) (in Japanese)